Multi-wavelength view and modeling of the blazar B2 1811+31 in flaring state

Davide Cerasole*

On behalf of MWL collaborators,
the MAGIC and Fermi-LAT Collaboration

V Gravi-Gamma-Nu Workshop 2024

Bari, October 10, 2024

* Dipartimento di Fisica 'M. Merlin' dell'Università e del Politecnico di Bari
Istituto Nazionale di Fisica Nucleare, Sezione di Bari
davide.cerasole@ba.infn.it

Istituto Nazionale di Fisica Nucleare
SEZIONE DI BARI

Dipartimento Interateneo di Fisica "M. Merlin"

Blazars

$$\upsilon F_{\upsilon} = E^2 \frac{dN_{\gamma}}{dE}$$

- **Blazars** are active galactic nuclei with jet aligned with our line of sight
  - **BL Lac objects** are blazars with **no or weak emission lines** in their **optical/UV spectra**
- Blazar broad-band spectral energy distribution (SED) shows non-thermal continuum from radio to γ rays with two main bumps

1. The first peaks at ν_{synch}, which varies from IR to X-rays.
   Dominated by **synchrotron emission by relativistic electrons** interacting with the magnetic field in the jet

• $\nu_{synch} < 10^{14}$ Hz	Low synchrotron-peaked (SP) BL Lacs (**LBL**)
• 10^{14} Hz $< \nu_{synch} < 10^{15}$ Hz	Intermediate SP BL Lacs (**IBL**)
• $\nu_{synch} > 10^{15}$ Hz	High SP BL Lacs (**HBL**)

2. The second bump peaks at energies from MeV to TeV.
   Less certain origin:
   - Inverse-Compton (IC) scattering of electrons off synchrotron photons (**SSC**), photons external from the jet (EC) (e.g. dusty torus, accreting disk, BLR, CMB…)
   - Proton synchrotron (PS) or γ-rays from $\pi^0 \rightarrow \gamma\gamma$ decay from photomeson production ($p\gamma \rightarrow N\pi$) or proton-proton collisions

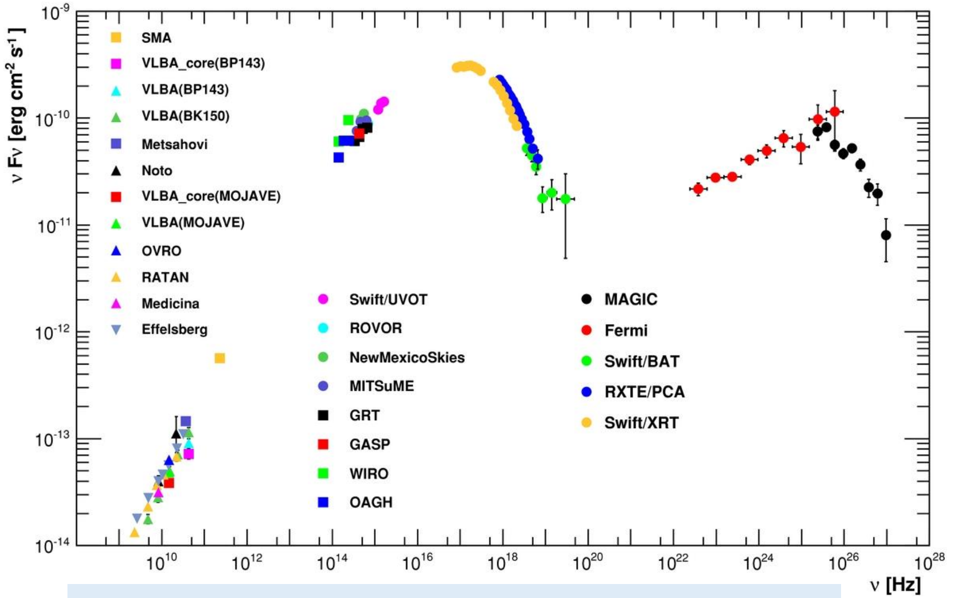

Broadband SED of the BL Lac Mrk 421 from a MWL campaign in 2009 (Abdo et al 2011)

Artistic view of a blazar emitting γ-rays and neutrinos (Credit IceCube - NASA - KM3NeT)

The MAGIC Telescopes

- System of two **Imaging Air Cherenkov Telescopes (IACTs)** located at the Observatorio del Roque de los Muchachos, La Palma Island, Canaries (2200 m a.s.l.)
    - 17 m diameter parabolic aluminum reflectors
    - PMT-based camera of ≈ 1000 pixels
    - Energy range **from 20 GeV** up **to 100 TeV**
    - **3.5° FoV**

Evolution of the integral sensitivity of MAGIC (Aleksic et al. 2016)

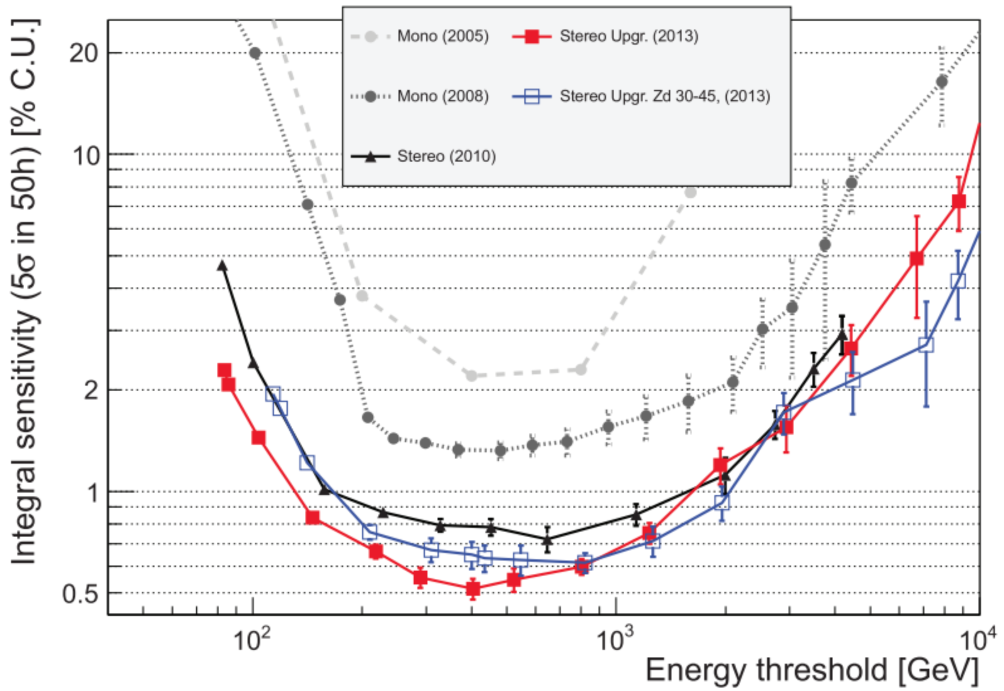

- Up to October 2024 (TeVCat), 88 AGNs detected ad TeV
    - 57 HBLs
    - 10 FSRQs
    - 10 IBLs
    - 2 LBLs
    - 4 blazars, 2 AGNs and 2 BL Lac objects of unclear type

Most VHE AGNs are HBLs

Very few LBLs and IBLs are detected at TeV

B2 1811+31

- $z = 0.117$ (Giommi et al. 1991, ApJ, 387, 77, tentative value)
- **Classified as IBL** in TeVCat
- ***Fermi*-LAT** observations of high state in HE γ rays led to a MWL campaign from radio to (VHE; 100 GeV < E < 100 TeV) γ rays
  - ATel #14060: *Fermi*-LAT detection of a hard-spectrum GeV flare from the BL Lac B2 1811+31 - 2 October 2020

- **MAGIC** announced the first detection of VHE γ-ray emission from B2 1811+31 on October 13, 2020
  - ATel #14090: Detection of very-high-energy gamma-ray emission from B2 1811+31 with the MAGIC telescopes

- Simultaneous MWL campaign during 2020 high state + long-term monitoring over 15 years, from 2008 to 2023
  - **HE** (*Fermi*-LAT) and **VHE γ rays** (MAGIC)
  - **Optical/UV** (*Swift*-UVOT) and **X rays** (*Swift*-XRT)
  - **Optical** (CRTS, KAIT, ZTF, Würzburg, KVA, Siena)
  - **Radio** (OVRO, TELAMON)

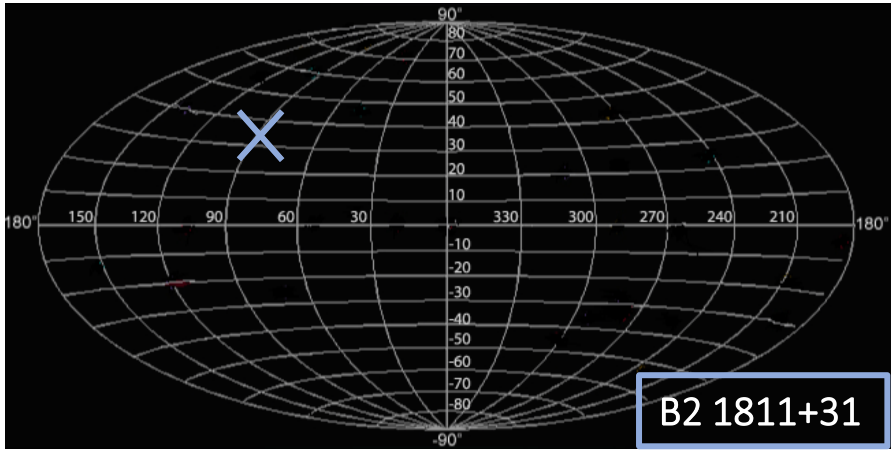


Fermi satellite

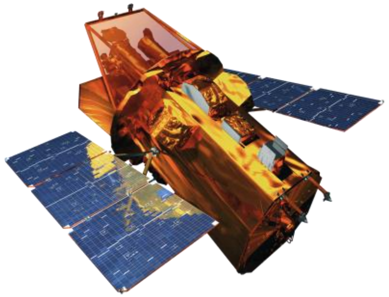
Swift satellite


MAGIC telescopes


OVRO

MAGIC detection of VHE emission from B2 1811+31

- Observations from October 5th to 11th, 2020
  - **5 nights of observations**
  - **Detection with 5.3 sigma**
- Night-wise gamma-ray flux for **energies above 135 GeV**
- Data from the last 3 observation nights, October 9-11, 2020, combined to evaluate the overall spectrum (see next slide)
- Unfolding for energy dispersion and correction for absorption by the **Extragalactic Background Light** (**EBL**)
- Intrinsic spectrum fitted with a **power-law** (**PL**) function
  - $\Gamma = 3.75 \pm 0.40$
  - $E_0 = 125.16$ GeV
  - $N_0 = (7.4 \ \pm 2.0) \times 10^{-10}$ TeV $^{-1}$ cm $^{-2}$ s $^{-1}$
  - $\frac{dN}{dE} = N_0 \left(\frac{E}{E_0}\right)^{-\Gamma}$

MAGIC lightcurve

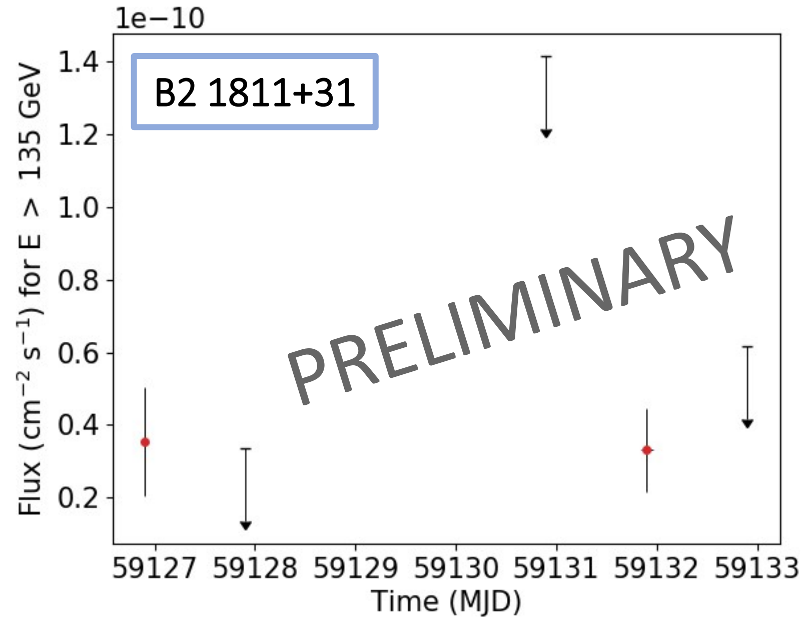

MAGIC SED

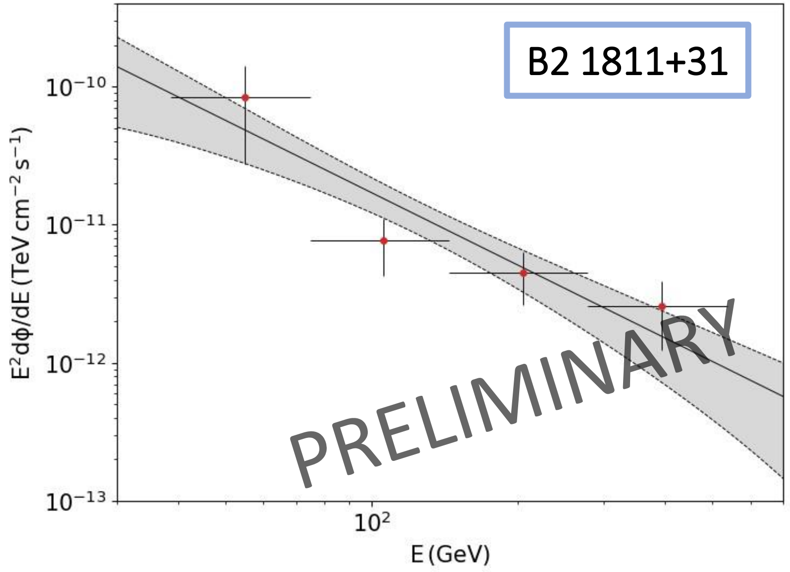

2020 flaring-state MWL lightcurve

- Fermi-LAT/Swift-UVOT data show that state during the first MAGIC observation nights (October 5-6, 2020, reddish band) differs from that during the last three MAGIC observations (October 9-11, 2020, blue band)

- The **daily gamma-ray variability** can be used to set a constraint on the **size of the emission region** responsible for the gamma-ray flare
    - Method in Foschini L. et al., A&A 530, A77(2011) consists in a lightcurve scan to find minimum doubling/halving time τ, $F(t) = F(t_0)2^{-(t-t_0)/\tau}$
- Upper limit to the emission size region moving with δ_D Doppler factor: $R \leq c\tau\frac{\delta_D}{1+z}$
- Observed variability of **3 – 6 hours** implies an upper limit of $(3-6)\times10^{14}\delta_D$ cm

Fermi-LAT trigger

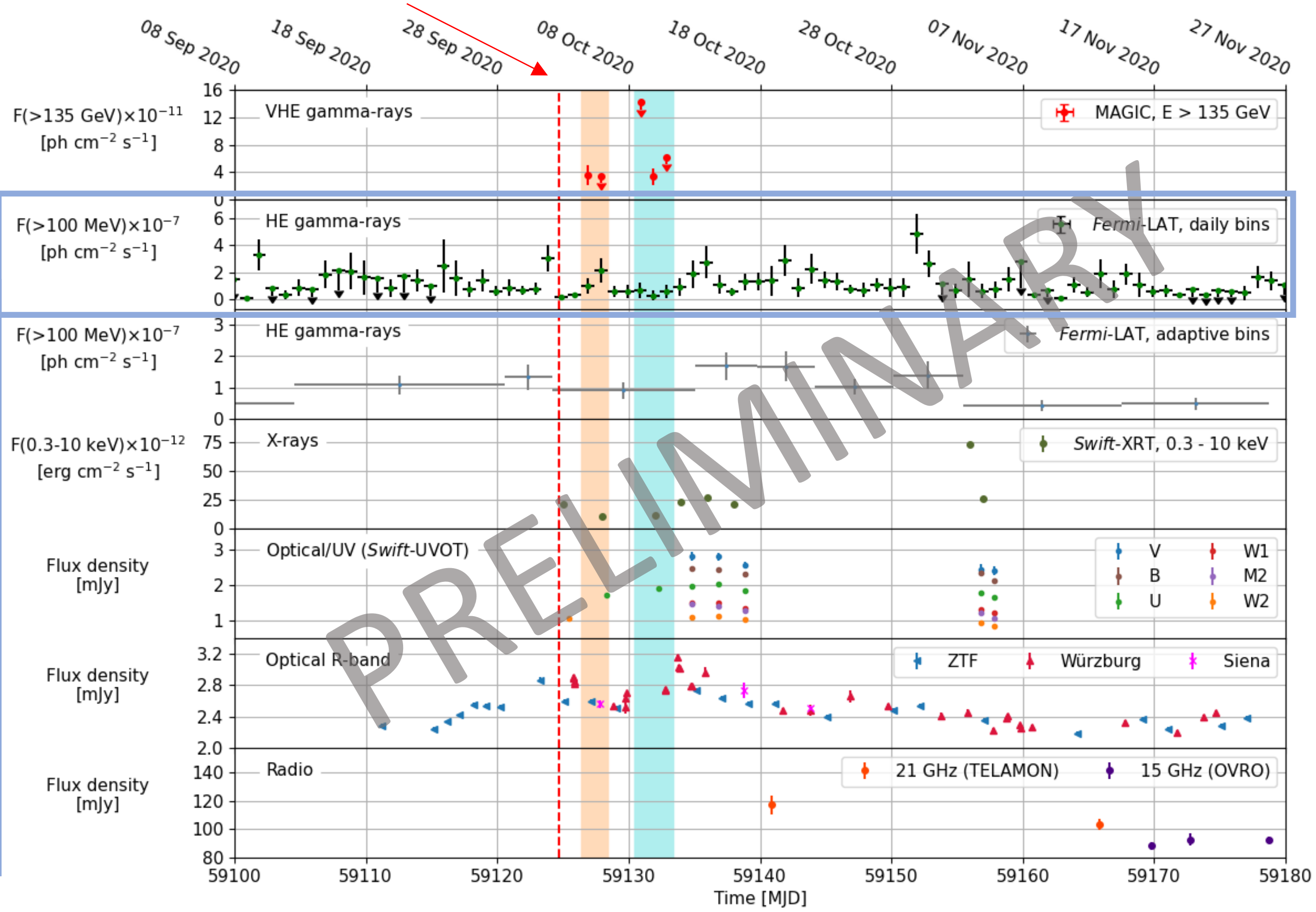

Long-term MWL lightcurve

- Coherent high state at **HE gamma-rays**, **X rays** and in **optical/UV**
- The 2020 HE γ-ray flare occurs at the apex of an increase in the **optical activity lasting for several years**
- **Hint of long-term correlation** with no delay of the **optical** and **γ-ray** lightcurves
  - Commonly found for FSRQs, LBLs and IBLs
- **Different trend** in long-term **radio** monitoring
  - Bulk of the emission in radio originated in regions different from those responsible for the high state in optical, X and γ-ray bands
- *Top panel*: shaded areas indicate the 'Pre-flare', 'Flare', and 'Post-flare' periods
  - Detailed HE γ-ray spectral analyses in these three periods are described in slide 11

Fermi-LAT trigger

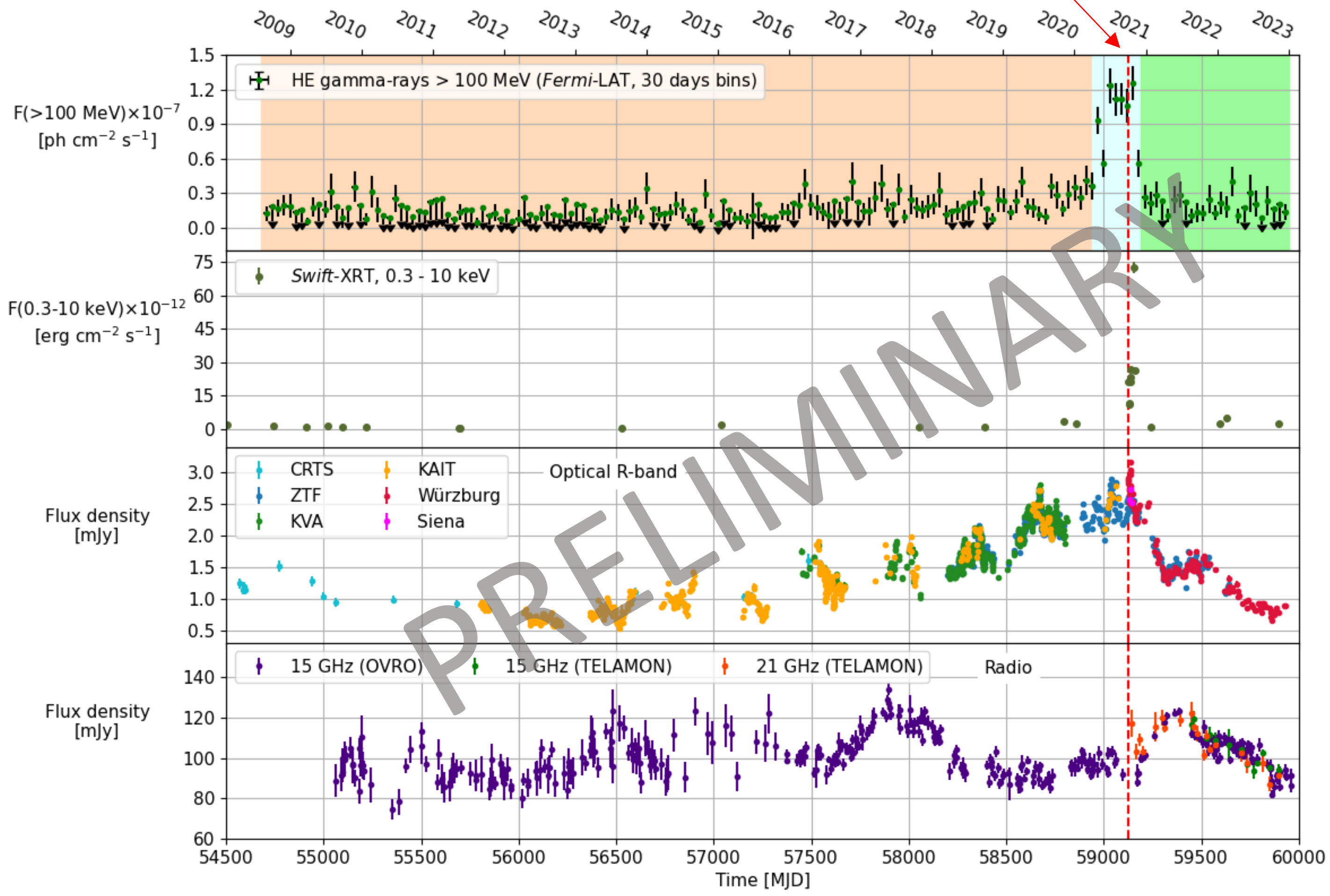

MWL cross-correlation analyses in slide 12

Long-term optical-to-X-ray SED evolution

- Long-term Swift-UVOT and Swift-XRT observations were employed to characterize the source variability in the **optical/UV** and **X-ray** bands.
- 2020 flare: **optical/UV** flux is a **factor 2 higher** than the values during the low state
- **X-ray variability over 2 decades** at 1 keV

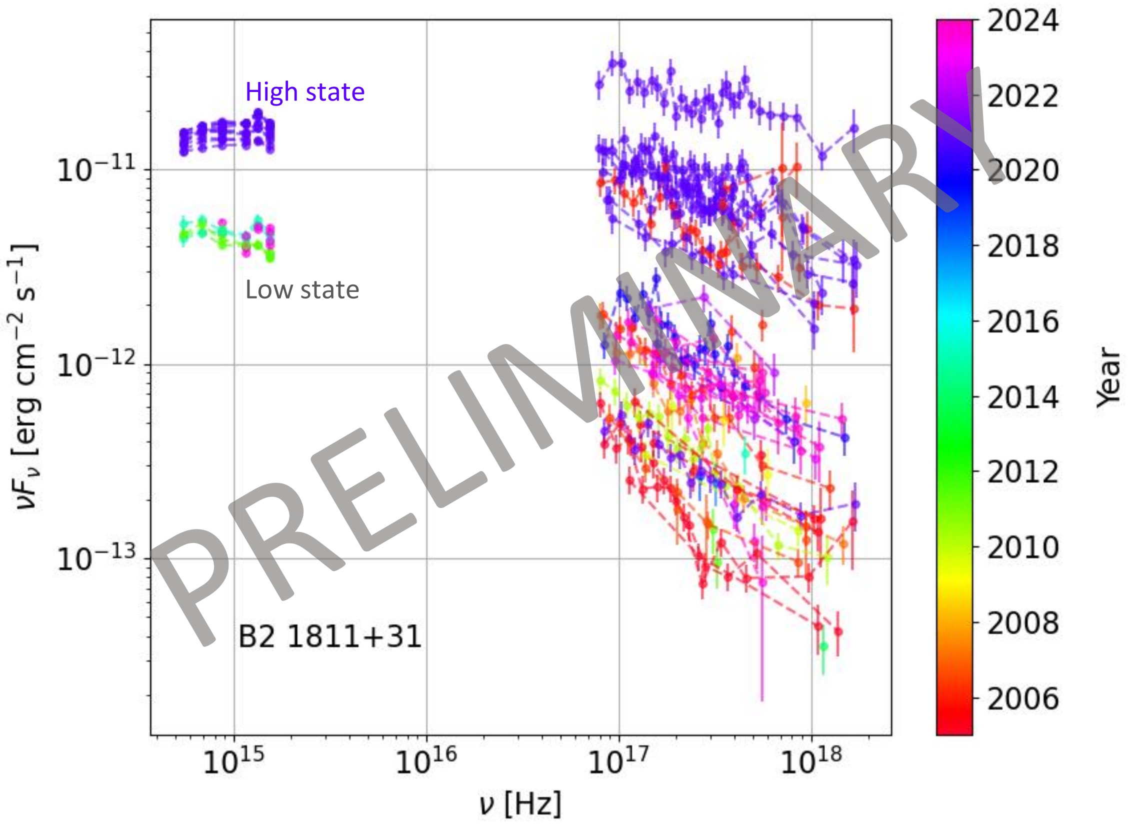

Long-term optical-to-X-ray SED evolution

- Long-term Swift-UVOT and Swift-XRT observations were employed to characterize the source variability in the **optical/UV** and **X-ray** bands.
- 2020 flare: **optical/UV** flux is a **factor 2 higher** than the values during the low state
- **X-ray variability over 2 decades** at 1 keV
- X rays: **harder-when-brighter trend**
  - Can be observed in blazars **with X-ray emission** dominated by the synchrotron radiation from the **highest energy electrons** accelerated in the jet
- Pearson $r = -0.77$ (p-val $= 2.2 \times 10^{-6}$) between X-ray spectral index and $\log F_X$
- Synchrotron emission from population of electrons $n_e(\gamma) \propto \gamma^{-p}$ has SED $\upsilon F_\upsilon \propto \upsilon^{\frac{3-p}{2}}$

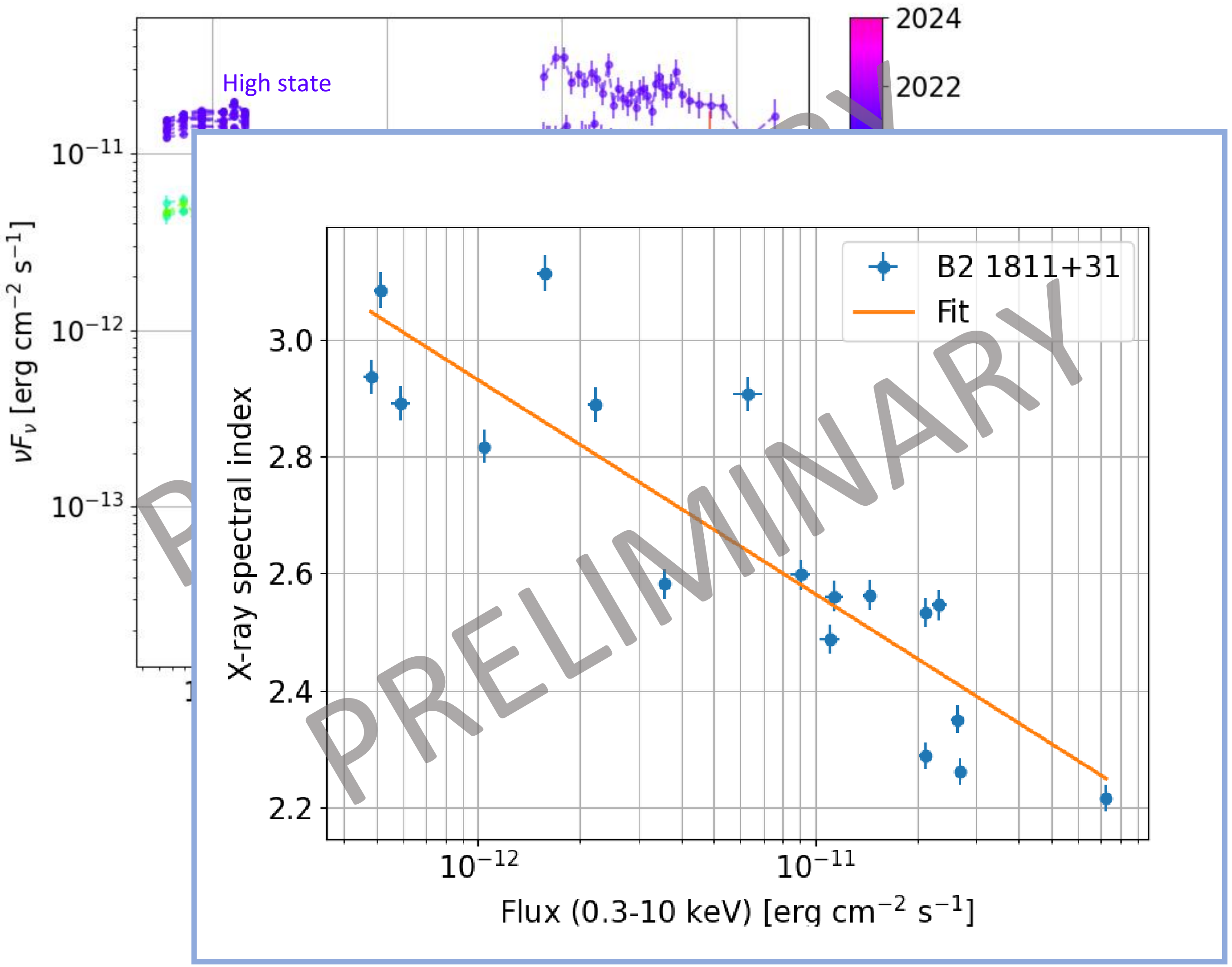

Low and high source states classification

- Simultaneous observations were used to **classify the source states** according to the **synchrotron peak frequency** ν_{synch}
- Quadratic function in the $\log_{10}\nu - \log_{10}F_\nu(\nu)$ space
  $$\nu\, F_\nu(\nu) = f_0\; 10^{-b\,(\log_{10}(\nu/\nu_{synch}))^2}$$
- Low state
  - $\nu_{synch} \approx 10^{14.71 \pm 0.03}$ Hz
  - **IBL during non-flaring state**
- 2020 high state
  - $\nu_{synch} \approx 10^{15.21 \pm 0.23}$ Hz
  - **Borderline between IBL/HBL during flaring state**

- Significant **shift upwards** in the **synchrotron peak frequency** during the 2020 **high state**

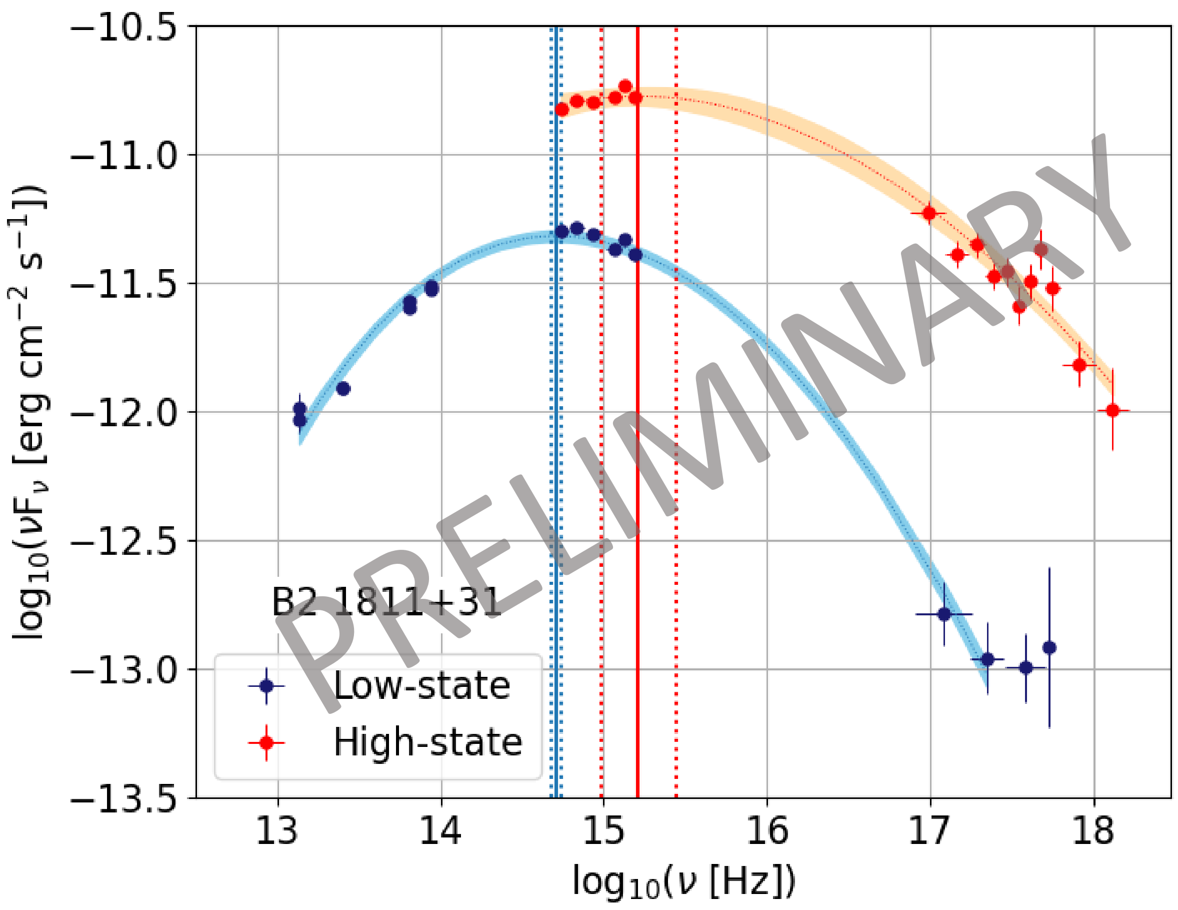

Long-term HE gamma-ray SED evolution

- Spectral analyses in the 100 MeV - 1 TeV range yield evidence for **strong spectral hardening** during the high-energy flare period in 2020
- **Peak frequency** of the **high-energy SED bump shifts to higher frequencies** during the flare, with spectral break lying likely at tens of GeV
- Signature of **freshly accelerated particles** in the jet encountering strong magnetic fields

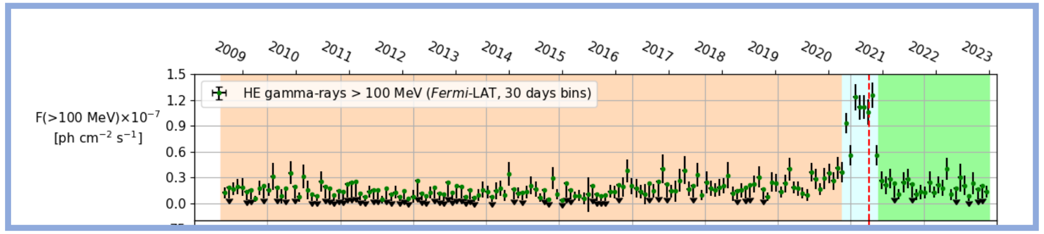

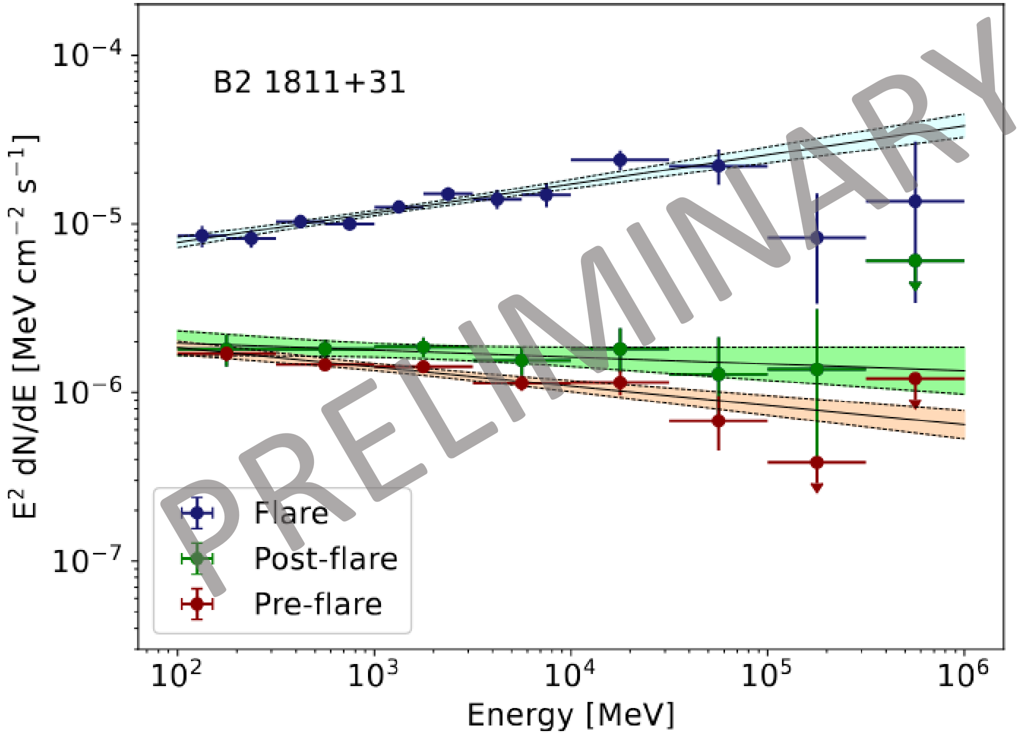

Period	Start [MJD]	Stop [MJD]	Γ_{PL}	F (>100 MeV)×10^{-8} [ph cm^{-2} s^{-1}]
Pre-flare	54682	58940	2.11 ± 0.03	1.7 ± 0.1
Flare	58940	59190	1.83 ± 0.02	9.6 ± 0.5
Post-flare	59190	59945	2.04 ± 0.05	1.9 ± 0.3

Multi-band cross-correlations

- These can be used to look for **signatures of multiple emission components** in the jet
- z-transformed Discrete Correlation Function (zDCF) to quantify correlation between
  - **HE γ rays**, **optical** R-band, **radio** 15 GHz
- Confidence levels (CLs) estimated simulating uncorrelated lightcurves following [Emmanoulopoulos D. et al. (2013)]
- Power Spectral Densities (PSDs) of the long-term lightcurves fitted with PLs: $PSD(\omega) = A\omega^{-\beta}$
  - $\beta_\gamma = 1.1$
  - $\beta_{\mathrm{R-band}} = 1.5$
  - $\beta_{\mathrm{Radio}} = 2.3$

- **HE γ rays/optical R-band** correlation with 95% CL
- **Radio not significantly correlated** with γ or optical

Summary of zDCF analyses. 1σ (3σ) band indicated in dark (light) gray.

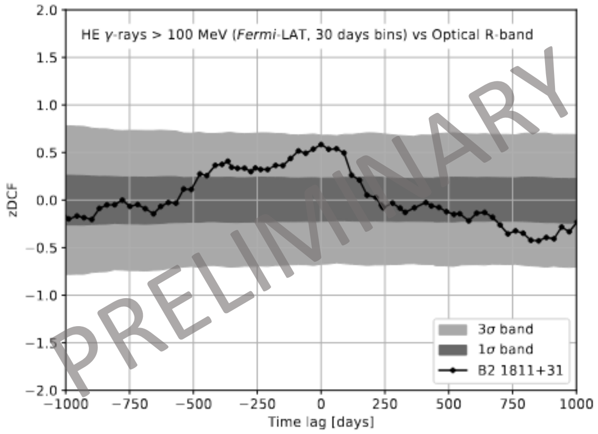

(a) zDCF of the long-term HE γ-ray and R-band light-curves.

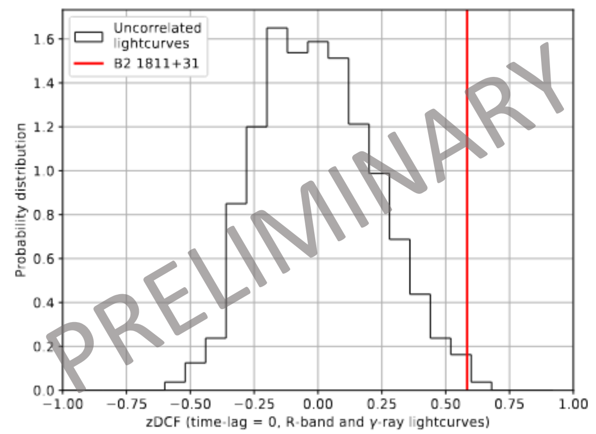

(b) Correlation with 95% CL of long-term γ-ray and R-band light-curves.

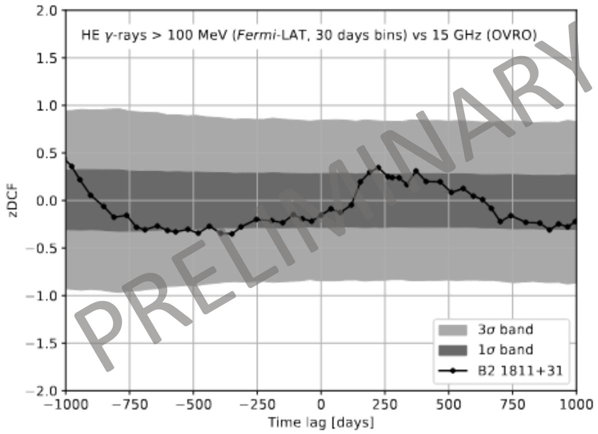

(c) zDCF of the long-term HE γ-ray and 15 GHz light-curves.

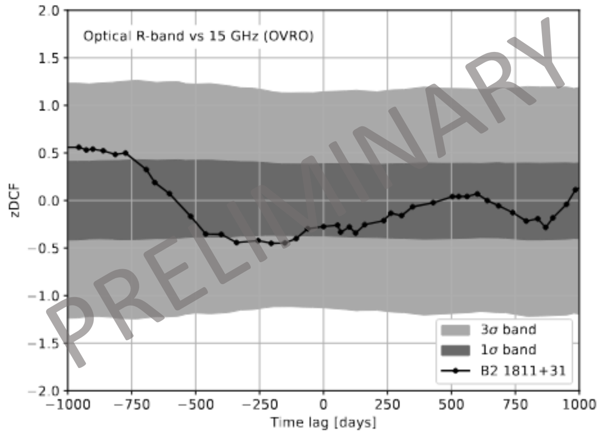

(d) zDCF of the long-term R-band and 15 GHz light-curves.

Summary and conclusions

- The blazar **B2 1811+31** entered the catalog of **TeV-detected** sources in 2020 thanks to the detection by the MAGIC telescopes, in a MWL campaign following the *Fermi*-LAT observations of high state
- B2 1811+31 behaved as **IBL in quiet state** and as **borderline IBL/HBL during the flaring state**
  - ISP BL Lacs are rare sources in the TeV sky
- MWL coverage from radio to VHE γ-rays during the high-state and analysis of long-term MWL data provide a unique way to investigate the **dynamics** and **emission mechanisms** of particles accelerated in the jet in both the **steady and flaring states**
- During the **2020 flare**, **both SED bumps** shifted to **higher flux levels** and **higher energies**
- The *Fermi*-LAT lightcurve showed **fast variability of few hours**, providing an UL of $\approx 6 \times 10^{14} \delta_{\mathrm{D}}$ cm to the size of the emission zone responsible for the γ-ray flare detected by the MAGIC telescopes
- **Multi-band cross-correlations** can act as guidance to the broad-band SED modelling

Thank you for your attention!